On the Performance of NOMA in SWIPT Systems with Power-Splitting Relaying

Huu Q. Tran[1,2], Tien-Tung Nguyen[2], Ca V. Phan[1], Quoc-Tuan Vien[3]
[1]Ho Chi Minh City University of Technology and Education, Vietnam.
Email: ttdv08@gmail.com/huutq.ncs@hcmute.edu.vn; capv@hcmute.edu.vn
[2]Industrial University of Ho Chi Minh City, Vietnam. Email: tranquyhuu@iuh.edu.vn; nguyentientung@iuh.edu.vn;
[3]Middlesex University, United Kingdom. Email: q.vien@mdx.ac.uk

Abstract—**This paper presents a decode-and-forward (DF) relaying protocol, namely power-splitting relaying (PSR), employed at relay nodes in NOMA technique. The PSR is considered for simultaneous wireless information and power transfer (SWIPT) systems. The relaying node is both energy harvesting from the received radio frequency (RF) signal and information forwarding to the destination. The outage performance and ergodic rate of the PSR are analyzed to realize the impacts of energy harvesting time, energy harvesting efficiency, power splitting ratio, source data rate, and the distance between the source and relay nodes. The simulation results show that NOMA schemes have the lower outage probability compared to the that of the conventional orthogonal multiple access (OMA) schemes at the destination node. Numerical results are provided to verify the findings.**

Index Terms—**Non-orthogonal multiple access, energy harvesting, power-splitting relaying, decode-and-forward, half-duplex.**

I. INTRODUCTION

Nowadays, energy harvesting (EH) and information processing (IP) have attracted many researchers [1] - [3]. Due to the limitation of the power storage, the EH in wireless relay and wireless sensor networks maybe need to be investigated [4], [5].

Several EH techniques and cooperative relay protocols have been embedded into the devices to prolong the network lifetime. such as SWIPT. In [6], a relaying protocol was proposed with the EH function where the relays replenish the energy from the received RF signals. In [7], a non-shared power allocation scheme and its performance were investigated and compared to several shared power allocation schemes.

The EH with a dual-hop half-duplex (HD) and full-duplex (FD) SWIPT employing both the DF and AF relaying was proposed in [8] for log-normal fading channels. In [9], a joint NOMA and partial relay selection was proposed to enhance both sum rate and user fairness while significantly decreasing outage probability. In [10], both FD and HD transmission modes were considered for an AF-based NOMA system. However, the adaptation of the EH and NOMA in SWIPT systems, to the scope of the authors' knowledge, has not yet investigated deeply in the literature.

In this paper, we study the employment of EH and DF-based NOMA in a SWIPT system. Based on [11], the PSR protocol with power splitting (PS) receiver architecture is considered in our work. In this protocol, the energy-constrained relay node uses a portion of the received power for energy harvesting and

the remaining energy for information processing. The main contributions of this paper can be summarized as follows:

- An HD NOMA scheme is proposed for a SWIPT system to allocate power for two users in which the one is considered as a relay node to perform both EH and DF the received signal. Thus, this scheme allows the PS receiver architecture to perform both information processing and energy harvesting at the relay node.
- The performance of the proposed scheme is analysed in terms of outage probability, throughput and ergodic rate. Specifically, closed-form expressions are derived for the outage probability at both users, while the analytical results of the throughput and ergodic rage are obtained for delay-limited and delay-tolerant transmission modes, respectively. It is shown that, with the NOMA adaptation, an enhanced outage performance is achieved for a considerably increased throughput and ergodic rage when compared to the conventional OMA.
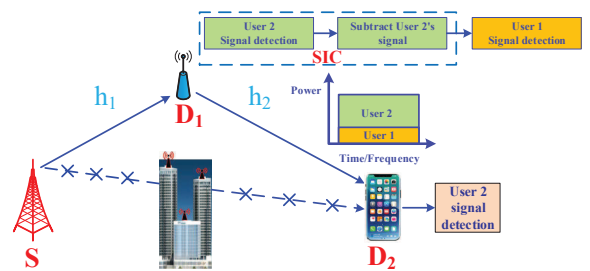
II. SYSTEM MODEL

Fig. 1: System Model.

Figure 1 illustrates the system model under investigation, in which a source node, S, wants to transfer the information to two users D_1 and D_2. It is assumed that there is an obstacle between S and D_2. As shown in Fig. 1, S sends data to D_1 and D_1 is exploited to assist the communications from S to D_2. Here, D_1 employs DF relaying protocol using the energy harvested from S. The distances from S to D_1 and from D_1 to D_2 are denoted by d_1 and d_2, respectively. The complex channel coefficients of $S \rightarrow D_1$ and $D_1 \rightarrow D_2$ links are denoted by h_1 and h_2, with respective power gains of $|h_1|^2$

and $|h_2|^2$, which are assumed to be exponentially distributed with $E[|h_1|^2] = \Omega_1^{-1}$ and $E[|h_2|^2] = \Omega_2^{-1}$. Here, E[.] denotes expectation operation.

A. Energy Harvesting at D_1

With the employment of superposition of the transmitted signals at S as in the NOMA scheme, the observation at D_1 is given by

$$y_{D_1} = h_1(\sqrt{a_1 P_s} x_1 + \sqrt{a_2 P_s} x_2) + n_{D_1}, \tag{1}$$

where P_s is transmission power at S, a_1 and a_2 are power allocation coefficients for data symbols x_1 and x_2 wished to send from S to D_1 and D_2, respectively. n_{D_1} is additive white Gaussian noise (AWGN) at D_1 with zero mean and variance σ^2. It is assumed that $E[x_1^2] = E[x_2^2] = 1$, and $a_2 > a_1 > 0$ satisfy $a_1 + a_2 = 1$ when lacking of loss of generality.

Employing PSR protocol, D_1 splits the received power into two parts including: i) harvested energy and ii) information processing energy. Let β, $0 < \beta < 1$, denotes the power splitting ratio. The energy harvested at D_1 can be obtained as

$$E_H = \beta \eta |h_1|^2 \rho (T/2), \tag{2}$$

where $\rho \overset{\Delta}{=} P_S / \sigma^2$ represents the transmit signal-to-noise ratio (SNR) and $0 < \eta < 1$ denotes the energy harvesting efficiency at the energy receiver which is dependent of the rectifier and the energy harvesting circuitry. All the energy harvested during energy harvesting phase is consumed at D_1 while forwarding the decoded signal to D_2.

From the harvested energy E_H, the transmission power at D_1 can be given by

$$P_r = \frac{E_H}{(T/2)} = \frac{\beta \eta |h_1|^2 \rho (T/2)}{(T/2)} = \beta \eta |h_1|^2 \rho. \tag{3}$$

B. Information Processing at D_1 and D_2

Applying the NOMA principle, D_2 is allocated more power than that for D_1. After receiving the signal from S, D_1 decodes the signal x_2 and decodes its own signal x_1 by employing successive interference cancellation (SIC) [12].

From (1) the received signal to interference plus noise ratio (SINR) at D_1 to detect x_2 of D_2 is given by

$$\gamma_{D_2 \rightarrow D_1} = \frac{\psi_I |h_1|^2 a_2 \rho}{\psi_I |h_1|^2 a_1 \rho + 1}, \tag{4}$$

where $\psi_I = (1 - \beta)$ denotes the information processing coefficient in the PSR protocol. After SIC, there is no interference remaining in the received signal at D_1. The received SNR at D_1 to detect its own message x_1 is thus given by

$$\gamma_{D_1} = \psi_I |h_1|^2 a_1 \rho. \tag{5}$$

Meanwhile, the decoded signal x_2 at D_1 is forwarded to D_2. The received signal at D_2 can be expressed as

$$y_{D_2} = (\sqrt{P_r} x_2) h_2 + n_{D_2}. \tag{6}$$

Substituting Eq. (3) into y_{D_2}, we obtain

$$y_{D_2} = (\sqrt{\beta \eta \rho}) h_1 h_2 x_2 + n_{D_2}. \tag{7}$$

The received SNR at D_2 is thus given by

$$\gamma_{2,D_2} = |h_2|^2 |h_1|^2 \psi_E \rho, \tag{8}$$

where $\psi_E = \beta \eta$ denotes the energy harvesting coefficient in the PSR protocol.

III. PERFORMANCE ANALYSIS

A. Outage Performance

1) Outage Probability at D_1: In the NOMA protocol, D_1 is not in outage when it can decode both x_1 and x_2 received from S. Therefore, the outage probability at D_1 can be expressed by

$$P_{D_1,PSR}^{HD} = 1 - \Pr\left(\gamma_{D_2 \rightarrow D_1} > \gamma_{th_2}^{HD}, \gamma_{D_1} > \gamma_{th_1}^{HD}\right), \tag{9}$$

where $\gamma_{th_1}^{HD} = 2^{2R_1} - 1$ and $\gamma_{th_2}^{HD} = 2^{2R_2} - 1$. Here, R_1 and R_2 are the target rates for detecting x_1 and x_2 at D_1, respectively. We present the following finding of the outage probability at D_1.

Theorem 1. *The outage probability at D_1 is given by*

$$P_{D1,PSR}^{HD} = 1 - e^{-\frac{\theta_1}{\Omega_1}}, \tag{10}$$

where $\theta_1 = \max(\tau_1, \nu_1), \tau_1 = \frac{\gamma_{th_2}^{HD}}{\rho \psi_I (a_2 - a_1 \gamma_{th_2}^{HD})}$ *and* $\nu_1 = \frac{\gamma_{th_1}^{HD}}{a_1 \psi_I \rho}$ *with* $a_2 > a_1 \gamma_{th_2}^{HD}$.

Proof: The outage probability at D_1 can be computed by

$$\begin{aligned} P_{D_1,PSR}^{HD} &= 1 - P_r\left(|h_1|^2 \geq \theta_1\right) \\ &= 1 - \int_{\theta_1}^{\infty} f_{|h_1|^2}(y) \, dy \\ &= 1 - e^{-\frac{\theta_1}{\Omega_1}}. \end{aligned} \tag{11}$$

The proof is completed. ∎

2) Outage Probability at D_2: Note that the far-end node D_2 is in outage when either D_1 can not detect x_2 or D_2 can not recover the forwarded signal from D_1. The outage probability at D_2 can be derived as in Eq. (12) (see the top of next page). Deriving J_2 and J_3, we have the following finding

Theorem 2. *The outage probability at D_2 can be given by*

$$P_{D_2,PSR}^{HD} = 1 - e^{-\frac{\tau_1}{\Omega_1}} +$$
$$\int_{\tau_1}^{\infty} \left(1 - e^{-\frac{\gamma_{th_2}^{HD}}{x \psi_E \rho \Omega_2}}\right) \frac{1}{\Omega_1} \exp\left(\frac{-x}{\Omega_1}\right) dx. \tag{13}$$

Proof: Considering Rayleigh fading channel, J_2 in Eq. (12) can be given by

$$J_2 = 1 - \exp\left(\frac{-\tau_1}{\Omega_1}\right). \tag{14}$$

and J_3 can be expressed as in Eq. (15) (see the top of next page).

$$P_{D_2,PSR}^{HD} = \underbrace{\Pr\left(\gamma_{D_2 \to D_1} < \gamma_{th_2}^{HD}\right)}_{J_2} + \underbrace{\Pr\left(\gamma_{2,D_2} < \gamma_{th_2}^{HD}, \gamma_{D_2 \to D_1} > \gamma_{th_2}^{HD}\right)}_{J_3}. \tag{12}$$

$$J_3 = \Pr\left(|h_2|^2 |h_1|^2 \psi_E \rho < \gamma_{th_2}^{HD}, \frac{|h_1|^2 \psi_I a_2 \rho}{\psi_I |h_1|^2 a_1 \rho + 1} > \gamma_{th_2}^{HD}\right) = \begin{cases} \Pr\left(|h_2|^2 < \dfrac{\gamma_{th_2}^{HD}}{|h_1|^2 \psi_E \rho}, |h_1|^2 > \dfrac{\gamma_{th_2}^{HD}}{\psi_I \rho\left(a_2 - a_1 \gamma_{th_2}^{HD}\right)}\right), & a_2 > a_1 \gamma_{th_2}^{HD} \\[2mm] 0, & a_2 \le a_1 \gamma_{th_2}^{HD} \end{cases}$$

$$= \int_{\frac{\gamma_{th_2}^{HD}}{\psi_I \rho\left(a_2 - a_1 \gamma_{th_2}^{HD}\right)}}^{\infty} \int_{0}^{\frac{\gamma_{th_2}^{HD}}{x \psi_E \rho}} f_{|h_1|^2}(x) f_{|h_2|^2}(y) \, dx \, dy = \int_{\tau_1}^{\infty} \frac{1}{\Omega_{1,PSR}} \left[1 - \exp\left(\frac{-\gamma_{th_2}^{HD}}{x \psi_E \rho \Omega_{2,PSR}}\right)\right] \exp\left(\frac{-x}{\Omega_{1,PSR}}\right) dx. \tag{15}$$

The outage probability at D_2 is given by

$$P_{D_2,PSR}^{HD} = J_2 + J_3 \tag{16}$$

∎

Corollary 1. *In the case of high SNR, the outage probability at D_2 can be derived as in Eq. (17) (see the top of next page), where $K_1(.)$ denote the first order modified Bessel function of the second kind* [13, Eq.(9.6.22)].

B. Throughput for Delay-limited Transmission Mode

In this mode, it is assumed that the source node transmits information with a constant rate of R, depending on the performance of the outage probability due to wireless fading channels. The system throughput of HD transmission mode in the NOMA system is thus given by

$$\tau_{t,PSR}^{HD} = \left(1 - P_{D_1,PSR}^{HD}\right) R_1 + \left(1 - P_{D_2,PSR}^{HD}\right) R_2, \tag{18}$$

where $P_{D_1,PSR}^{HD}$ and $P_{D_2,PSR}^{HD}$ can be obtained from (10) and (16), respectively.

C. Ergodic Rate for Delay-tolerant Transmission Mode

1) Ergodic Rate at D_1: For the case when D_1 can detect x_2, the achievable rate at D_1 can be written as

$$R_{D_1,PSR} = \frac{1}{2} \log_2\left(1 + \gamma_{D_1}\right). \tag{19}$$

The ergodic rate of D_1 for HD transmission mode in the NOMA system can be obtained by the following theorem.

Theorem 3. *The ergodic rate at D_1, is given by*

$$R_{D_1,PSR}^{HD} = \frac{-\exp\left(\frac{1}{\psi_I a_1 \rho \Omega_1}\right)}{2 \ln 2} Ei\left(\frac{-1}{\psi_I a_1 \rho \Omega_1}\right). \tag{20}$$

$Ei(x)$ *denotes the exponential integral function* [14, Eq.(3.352.4)].

Proof: See Appendix A. ∎

2) Ergodic Rate at D_2: Since x_2 needs to be detected at both D_1 and D_2, the achievable rate at D_2 for HD transmission mode in the NOMA system can be written as

$$R_{D_2,PSR} = \frac{1}{2} \log_2\left(1 + \min\left(\gamma_{D_2 \to D_1}, \gamma_{2,D_2}\right)\right). \tag{21}$$

Theorem 4. *The ergodic rate at D_2 is given by*

$$R_{D_2,PSR}^{HD} = \frac{1}{2 \ln 2} \int_{0}^{\frac{a_2}{a_1}} \left[\frac{e^{-\frac{x}{\psi_I \rho(a_2 - a_1 x)\Omega_1}}}{1 + x} \right. $$
$$\left. + \frac{\int_{\frac{x}{\psi_I \rho(a_2 - a_1 x)}}^{\infty} \frac{1}{\Omega_1}\left(1 - e^{-\frac{x}{y \rho \psi_E \Omega_2}}\right) e^{-\frac{y}{\Omega_1}} dy}{1 + x} \right] dx. \tag{22}$$

Proof: See Appendix B. ∎

3) Ergodic rate of the system: The system ergodic rate of HD transmission mode in the NOMA system is thus given by

$$\tau_{r,PSR}^{HD} = R_{D_1,PSR}^{HD} + R_{D_2,PSR}^{HD}, \tag{23}$$

where $R_{D_1,PSR}^{HD}$ and $R_{D_2,PSR}^{HD}$ can be obtained from (20) and (22), respectively.

IV. SIMULATION RESULTS

This section verifies the derived analytical results contained in the preceding sections. The values of the parameters set in our model are listed as follows: $d = 0.4$, $m = 2$, $a_1 = 0.2$, $a_2 = 0.8$, $R_1 = 3$ bps, $R_2 = 0.5$ bps where d is the normalized distance between the S and D_1; $\Omega_{SD_2} = 1$, $\Omega_{SD_1} = d^{-m}$ and $\Omega_{D_1 D_2} = (1-d)^{-m}$ are the distances normalized to unity; m is the pathloss exponent and Ri ($i = 1, 2$) are target rates, respectively.

In the simulation, the performance of the conventional OMA is used as a benchmark for comparison. Specifically, in the OMA scheme, S sends the information x_1 to user relay D_1 in the first time slot and sends x_2 to D_1 in the second time slot. Then, D_1 decodes and forwards the information x_2 to D_2 in the third time slot.

$$P_{D_2,PSR}^{HD,\infty} = \Pr\left(\frac{a_2}{a_1} < \gamma_{th_2}^{HD}\right) + \Pr\left(|h_2|^2 < \frac{\gamma_{th_2}^{HD}}{\psi_E \rho |h_1|^2}, \frac{a_2}{a_1} > \gamma_{th_2}^{HD}\right)$$

$$= \Pr\left(|h_2|^2 < \frac{\gamma_{th_2}^{HD}}{\psi_E \rho |h_1|^2}, \frac{a_2}{a_1} > \gamma_{th_2}^{HD}\right) \int_0^\infty \left[1 - \exp\left(\frac{-\gamma_{th_2}^{HD}}{\psi_E \rho \Omega_2 x}\right)\right] \frac{1}{\Omega_1} \exp\left(\frac{-x}{\Omega_1}\right) dx = 1 - 2\sqrt{\frac{\gamma_{th_2}^{HD}}{\psi_E \rho \Omega_1 \Omega_2}} K_1\left(2\sqrt{\frac{\gamma_{th_2}^{HD}}{\psi_E \rho \Omega_1 \Omega_2}}\right). \quad (17)$$

Figure 2 illustrates the outage probability of two users for the PSR protocol versus SNR. It can be observed that User 2 has a lower outage probability than that of User 1 in the HD NOMA scheme as well as in the HD OMA scheme. Also, the outage probability of two users in the HD NOMA scheme is shown to be lower than those in the HD OMA scheme. Moveover, the exact outage probability curves match precisely with the simulation results.
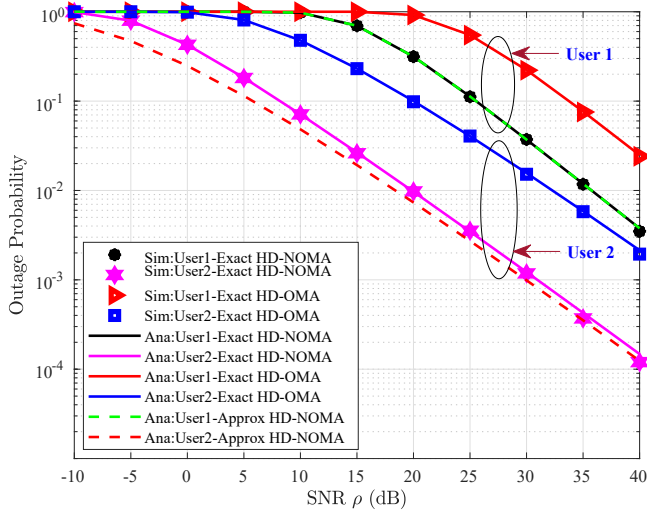

Fig. 2: Outage probability of two users for the PSR protocol versus transmitting SNR.

Considering the system throughput for delay-limited transmission mode and ergodic rate for delay-tolerant transmission mode, Figs 3, 4 sequentially represent throughput and the ergodic rate of two users for the PSR protocol versus β. Specifically, it can be seen in Fig. 3 that the throughput of User 1 is significantly higher than that of User 2 in the HD NOMA scheme. In contrary, the throughput of User 1 is lower than that of User 2 in the HD OMA scheme. This is due to the fact that D_1 receives both x_1 and x_2 signals while D_2 receives only x_2 in the delay-limited transmission mode. A similar observation can be realised in Figure 4. Compared with ergodic among the scheme, we can realzed that the ergodic rate at User 1 in the HD NOMA scheme is shown to be the highest, while the one at User 2 in the HD OMA scheme is the lowest.

This is because SNR at D_1 to detect x_1 and x_2 in equations (19), (20) which is higher than the minimum value of SNR at D_1 to detect x_2 and SNR at D_2 to detect x_2 in equations (22), (22).
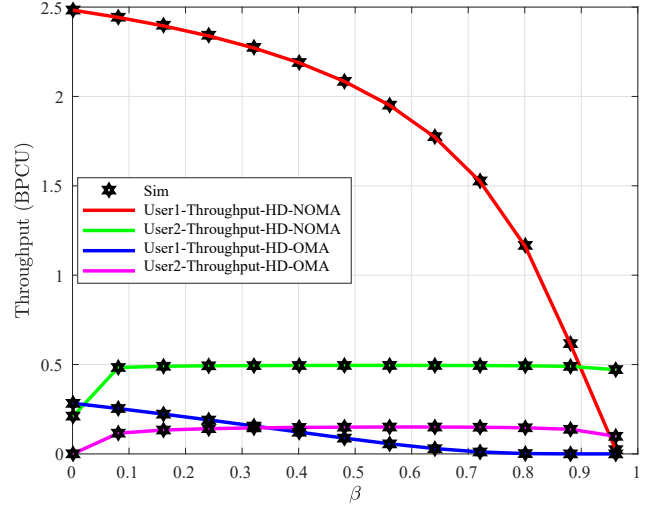

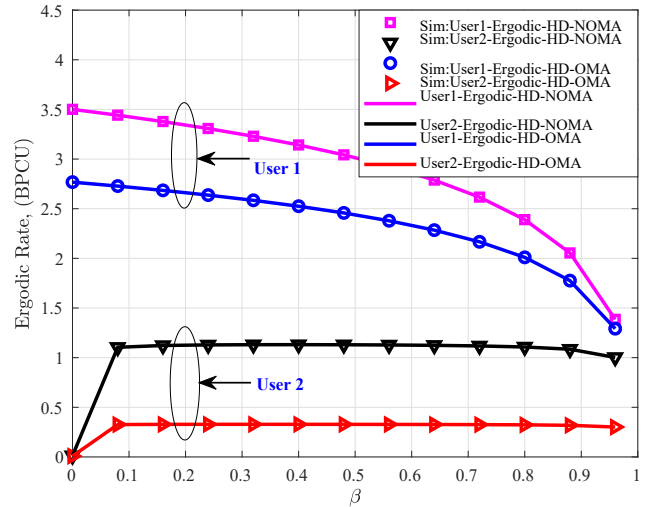Fig. 3: The throughput of two users for the PSR protocol versus β.

Fig. 4: The ergodic rate of two users for the PSR protocol versus β.

V. CONCLUSION

In this paper, an EH scheme has been proposed along with the adaptation of NOMA for a SWIPT system. A PSR has been employed for the DF relaying protocol. The closed-form expressions of outage probability as well as expressions of

the achievable throughput, ergodic sum rate at two users have been derived for the PSR and PSR protocol with joint EH and NOMA. The analytical results show that the NOMA achieves a lower outage probability at the far-end user when compared with the conventional OMA. Parallelly, numerical results show that NOMA has throughput and ergodic rate outperformed than when compared to the conventional OMA.

VI. APPENDICES

A. Appendix A

In this appendix, we present the proof of (20). To obtain this closed-form expression, the ergodic rate of D_1 for HD NOMA can be written as

$$R_{D_1,PSR}^{HD} = \frac{1}{2}\mathrm{E}\left[\log_2\left(1+\psi_I|h_1|^2 a_1\rho\right)\right] = \frac{1}{2\ln2}\int_0^\infty \frac{1-F_X(x)}{1+x}dx \tag{24}$$

The cumulative distribution function (CDF) of X is calculated as

$$F_X(x) = \Pr\left(|h_1|^2 < \frac{x}{\psi_I a_1\rho}\right)\int_0^{\frac{x(z\rho+1)}{\psi_I a_1\rho}}\frac{1}{\Omega_1}e^{-\frac{y}{\Omega_1}}dy$$
$$= 1 - e^{-\frac{x}{\psi_I a_1\rho\Omega_1}} \tag{25}$$

By replacing (25) in (24), the ergodic rate at D_1 can be derived as

$$R_{D_1,PSR}^{HD} = \frac{1}{2}\frac{1}{\ln2}\int_0^\infty\frac{1}{1+x}e^{-\frac{x}{\psi_I a_1\rho\Omega_1}}dx = \frac{-\exp\left(\frac{1}{\psi_I a_1\rho\Omega_1}\right)}{2\ln2}Ei\left(\frac{-1}{\psi_I a_1\rho\Omega_1}\right)$$

We can derive (20). The proof is completed.

B. Appendix B

In this appendix, the proof begins by giving the ergodic rate at D_2 as follows

$$R_{D_2,PSR}^{HD} = E\left[\frac{1}{2}\log_2\left(1+\underbrace{\min\left(\gamma_{D_2\to D_1},\gamma_{2,D_2}\right)}_{J_1}\right)\right]$$

$$J_1 = \underbrace{\min\left(\frac{\psi_I|h_1|^2 a_2\rho}{\psi_I|h_1|^2 a_1\rho+1},|h_2|^2|h_1|^2\psi_E\rho\right)}_{Y}$$

The CDF of Y is calculated as follows

$$F_Y(x) = I_3 + I_4 \tag{26}$$

where

$$I_3 = \Pr\left(\frac{\psi_I|h_1|^2 a_2\rho}{\psi_I|h_1|^2 a_1\rho+1} < |h_2|^2|h_1|^2\psi_E\rho, \frac{\psi_I|h_1|^2 a_2\rho}{\psi_I|h_1|^2 a_1\rho+1} < x\right) \tag{27}$$
$$= U\left(\frac{a_2}{a_1}-x\right)\int_0^{\overline{\frac{x}{\psi_I\rho(a_2-a_1x)}}}\frac{1}{\Omega_1}e^{-\frac{\psi_I a_2}{(\psi_I y a_1\rho+1)\psi_E\Omega_2}-\frac{y}{\Omega_1}}dy$$

and

$$I_4 = \Pr\left(\frac{\psi_I|h_1|^2 a_2\rho}{\psi_I|h_1|^2 a_1\rho+1} > |h_2|^2|h_1|^2\psi_E\rho, |h_2|^2|h_1|^2\psi_E\rho < x\right)$$
$$= \int_0^{\overline{\frac{x}{\psi_I\rho(a_2-a_1x)}}}\frac{1}{\Omega_1}\left(1-e^{-\frac{\psi_I a_2}{(\psi_I y a_1\rho+1)\psi_E\Omega_2}}\right)e^{-\frac{y}{\Omega_1}}dy$$
$$= \int_{\frac{x}{\psi_I\rho(a_2-a_1x)}}^\infty\frac{1}{\Omega_1}\left(1-e^{-\frac{y}{y\rho\psi_E\Omega_2}-\frac{y}{\Omega_1}}\right)dy. \tag{28}$$

The CDF of Y is given by

$$F_Y(x) = U\left(\frac{a_2}{a_1}-x\right)\left[1-e^{-\frac{x}{\psi_I\rho(a_2-a_1x)\Omega_1}}+\right.$$
$$\left.\int_{\frac{x}{\psi_I\rho(a_2-a_1x)}}^\infty\frac{1}{\Omega_1}\left(1-e^{-\frac{x}{y\rho\psi_E\Omega_2}}\right)e^{-\frac{y}{\Omega_1}}dy\right], \tag{29}$$

where $U(x)$ is unit step function. By replacing (29) into (21), we can obtain (22). The proof is completed.

REFERENCES

[1] R. Zhang and C. K. Ho, "MIMO broadcasting for simultaneous wireless information and power transfer," *IEEE Transactions on Wireless Communications*, vol. 12, no. 5, pp. 1989-2001, 2013.

[2] P. Popovski, A. M. Fouladgar, and O. Simeone, "Interactive joint transfer of energy and information," *ArXiv Technical Report*, 2012.

[3] Z. Xiang and M. Tao, "Robust beamforming for wireless information and power transmission," *IEEE Wireless Communications Letters*, vol. 1, no. 4, pp. 372375, 2012.

[4] P. T. Venkata, S. N. A. U. Nambi, R. V. Prasad, and I. Niemegeers, "Bond graph modeling for energy-harvesting wireless sensor networks," *IEEE Computer Society*, vol. 45, no. 9, pp. 3138, Sep. 2012.

[5] B. Medepally and N. B. Mehta, "Voluntary energy harvesting relays and selection in cooperative wireless networks," *IEEE Trans. Wireless Commun*, vol. 9, no. 11, pp. 35433553, Nov. 2010.

[6] Yanju Gu; Sonia Assa, "RF-based Energy Harvesting in Decode-and-Forward Relaying Systems: Ergodic and Outage Capacities," *IEEE Transactions on Wireless Communications*, vol. 14, no. 11, 2015.

[7] Lina Elmorshedy; Cyril Leung, "Power Allocation in an RF Energy Harvesting DF Relay Network in the Presence of an Interferer," *IEEE Access*, vol. 5 , pp. 7606 7618, 2017.

[8] Khaled Maaiuf Rabie, Bamidele Adebisi, Mohamed-Slim Alouini, "Half-Duplex and Full-Duplex AF and DF Relaying With Energy-Harvesting in Log-Normal Fading," *IEEE Transactions on Green Communications and Networking*, vol. 1, no. 4, 2017.

[9] S. Lee, D. B. da Costa, Q.-T. Vien, T. Q. Duong, and R. T. de Sousa Jr, "Non-orthogonal multiple access schemes with partial relay selection," *IET Communications*, vol. 11, no. 6, pp. 846-854, 2017.

[10] Xinwei Yue, Yuanwei Liu, Shaoli Kang, Arumugam Nallanathan, and Zhiguo Ding, "Exploiting Full/Half-Duplex user relaying in NOMA systems," *IEEE Computer Society*, vol. 66, no. 2, pp. 560-575, 2018.

[11] X. Zhou, R. Zhang, and C. K. Ho, "Wireless information and power transfer: Architecture design and rate-energy tradeoff," *IEEE Transactions on Communications*, vol. 61, no. 11, pp. 4754-4767, 2012.

[12] Y. Wang, B. Ren, S. Sun, S. Kang, and X. Yue, "Analysis of Non-Orthogonal Multiple Access for 5G," *China Commun.*, vol. 13, no. 2, pp. 52-66, 2016.

[13] S. Luo, R. Zhang, and T. J. Lim, "Optimal save-then-transmit protocol for energy harvesting wireless transmitters," *Transactions on Wireless Communications*, vol. 13, no. 3, pp. 1196-1207, 2013.

[14] Abramowitz, M., Stegun, I.A, "Handbook of mathematical functions with formulas, graphs, and mathematical tables," *Dover, New York*, 1972

[15] Gradshteyn, I.S., Ryzhik, I.M, "Table of integrals, series and products," *Academic, San Diego, CA*, 6th edn, 2000.